URSI-B EMTS 2025, Bologna, 23–27 June

Numerical Solution of the GO Equations for GRIN Lens Antennas by Using the Lax-Friedrichs Sweeping Method

Ilir Gashi(1), Stefano Maci(1), and Matteo Albani(1)
(1) University of Siena, Department of Information Engineering and Mathematics, Siena, 53100, Italy

Abstract

This paper introduces a novel method for analyzing inhomogeneous lenses by numerically solving the Eikonal and transport equations on a computational grid, eliminating the need for ray tracing. The approach employs the sweeping method, a numerical technique that iteratively solves the governing equations across the grid. By alternating the traversal directions and incorporating Gauss-Seidel updates, the method ensures convergence while accounting for boundary conditions and neighboring grid values. The proposed algorithm, known as the Lax-Friedrichs Sweeping Method (LFSM), offers an efficient solution to the factored Eikonal and transport equations. It enables highly accurate computation of the Eikonal Laplacian, which significantly improves amplitude accuracy. This method outperforms traditional ray-tracing techniques in terms of speed, precision, computational efficiency, and robustness. The inputs required for LFSM-based GRIN lens analysis include a computational grid, a refractive index map, and the type and position of the source. The implementation of the LFSM is here presented, as well as the application of it to the analysis of a Maxwell fish eye lens.

1 Introduction

The growing demand for higher data rates and reduced latency in 5G communication networks has driven research into millimeter-wave (mm-wave) frequencies, offering broader bandwidths but introducing challenges such as high free-space path loss. To address these challenges, advanced antenna technologies with high directivity and multibeam capabilities are essential. Graded Index (GRIN) lens antennas have emerged as a promising alternative, offering advantages like compactness, cost-effective fabrication through additive manufacturing, and enhanced design flexibility. GRIN lenses can achieve beam scanning by adjusting the source's position relative to the lens, enabling multifocal and multibeam functionalities through customized refractive index distributions.
The renewed interest in GRIN lenses is closely tied to advancements in their fabrication using 3D printing technologies [1, 2, 3, 4]. Among the most widely utilized GRIN lenses are the spherical Luneburg lens (LL) [5] and the Maxwell fish-eye (MFE) lens [6], both of which have refractive indices expressible in analytical closed forms. However, their large and bulky designs pose challenges for certain applications.
To address these limitations, innovative flat cylindrical GRIN lenses have been developed through various approaches, including Transformation Optics (TO) [7], ray-tracing optimization [8], and analytical formulations based on geometrical optics (GO) [9, 10]. These methods are often tailored to specific applications, and they suffer by intrinsical limitations, which bound their applicability.
A novel approach on analyzing GRIN lenses is by resorting to sweeping methods [11, 12, 13], that are iterative algorithms designed to solve steady-state problems of hyperbolic partial differential equations, particularly Hamilton–Jacobi equations, which include the Eikonal and transport equations, that are the fundamental GO equations used for the analysis of GRIN lens antennas.
In this context, the Lax-Friedrichs Sweeping Method (LFSM) [14] offers a robust and efficient numerical approach for solving the factored Eikonal and transport equations.. Unlike traditional ray tracing, LFSM iteratively updates solutions over a computational grid by leveraging the causality of Hamilton–Jacobi equations. By alternating directional sweeps (e.g., left-to-right, top-to-bottom, right-to-left, bottom-to-top), LFSM ensures accurate and stable convergence, even in the presence of complex geometries or GO singularities like caustics. The use of factorization techniques in LFSM separates singular components from smooth ones, enabling precise computation of the amplitude distribution. This makes LFSM particularly effective for analyzing GRIN lens antennas with high refractive index gradients or irregular geometries, where conventional ray-tracing methods may struggle.
This paper focuses on the application of LFSM for GRIN lens antenna analysis, highlighting its advantages over traditional methods. The method is explained and the analysis of an Maxwell fish eye lens is presented, demonstrating the effectiveness of the proposed approach.

2 The Lax-Friedrichs Sweeping Method

The propagation of wavefronts through a medium with a varying refractive index is governed by the Eikonal equation, a partial differential equation expressed as:

$$|\nabla\Psi(\mathbf{r})| = n(\mathbf{r}), \tag{1}$$

where $\Psi(\mathbf{r})$ is the phase function, $n(\mathbf{r})$ denotes the refractive index at position $\mathbf{r} \in \Omega$, and $|\nabla\Psi(\mathbf{r})|$ is the gradient magnitude of Ψ at that point. To approximate the amplitude of the electric field, the transport equation is used:

$$\nabla\Psi(\mathbf{r}) \cdot \nabla|\mathbf{E}(\mathbf{r})| + \frac{1}{2}|\mathbf{E}(\mathbf{r})|\nabla^2\Psi(\mathbf{r}) = 0, \qquad (2)$$

where $|\mathbf{E}(\mathbf{r})|$ represents the amplitude of the electric field at $\mathbf{r}$. To solve equations (1) and (2), the Lax-Friedrichs Sweeping Method (LFSM) [14] is employed, in the $x-y$ plane. Readers can refer to [14] for detailed algorithmic implementation. Here we introduce the 2D case.

In a generalized form, the equations can be framed using the Hamiltonian:

$$H(x,y,u,u_x,u_y) = f(x,y), \qquad (3)$$

where u is the unknown variable, u_x and u_y are partial derivatives of u with respect to x and y, respectively, and $f(x,y)$ is a forcing term. The Hamiltonian equation is solved on a rectangular grid with uniform spacing h in both directions. Using a Gauss-Seidel-based sweeping scheme, the algorithm iteratively updates, in four different directions, the grid values until a predefined convergence criterion is satisfied. The accuracy of the solution improves with increased grid density.

To achieve high precision in computing the Laplacian term $\nabla^2\Psi$, a third-order sweeping scheme is utilized. This order is selected based on the required accuracy for the amplitude calculation through (2).

For point sources, which exhibit singularities in GO, accurate computation near the source region is achieved by employing a factored representation of the Eikonal and amplitude. In the vicinity of these sources, the field distribution can be approximated to that of a point source in free space. The refractive index and eikonal are factorized as:

$$\begin{cases} n(\mathbf{r}) = n_0(\mathbf{r})n_1(\mathbf{r}), \\ \Psi(\mathbf{r}) = \Psi_0(\mathbf{r})\Psi_1(\mathbf{r}), \end{cases} \qquad (4)$$

where Ψ_0 is the known phase function in a medium characterized by $n_0(\mathbf{r})$, satisfying $|\nabla\Psi_0(\mathbf{r})|^2 = n_0^2(\mathbf{r})$, and $n_1(\mathbf{r})$ is a smooth function with continuous first and second derivatives. A simple example is free-space propagation, where $n_0(\mathbf{r}) = 1$ and $\Psi_0(\mathbf{r}) = \sqrt{x^2+y^2} = \rho$.

By substituting (4) in (1), and by considering $n_0(\mathbf{r}) = 1$, the factored Eikonal equation is obtained:

$$\sqrt{\Psi_0^2|\nabla\Psi_1|^2 + 2\Psi_0\Psi_1(\nabla\Psi_0 \cdot \nabla\Psi_1) + \Psi_1^2} = n, \qquad (5)$$

where dependencies on $\mathbf{r}$ are implied for simplicity. Here, Ψ_0 accounts for the singular behavior at the source, ensuring that Ψ_1 remains smooth.

Similarly, the amplitude is factorized as:

$$A(\mathbf{r}) = A_0(\mathbf{r})A_1(\mathbf{r}), \qquad (6)$$

where $A_0(\mathbf{r})$ represents the free-space amplitude associated with $\Psi_0(\mathbf{r})$, and $A_1(\mathbf{r})$ is the unknown term to be determined. Substituting this factorization into the transport equation (2), the modified equation becomes:

$$\begin{aligned} &A_0\big(\Psi_0\nabla\Psi_1 + \Psi_1\nabla\Psi_0\big) \cdot \nabla A_1 \\ &\quad + \big(\Psi_0\nabla\Psi_1 \cdot \nabla A_0 + A_0\nabla\Psi_0 \cdot \nabla\Psi_1 + \frac{1}{2}A_0\Psi_0\nabla^2\Psi_1\big)A_1 = 0. \end{aligned} \qquad (7)$$

Using the sweeping method, the Hamiltonian (3), with $u = \Psi_1$, for the factored Eikonal equation (5) is expressed as:

$$\begin{cases} H = \sqrt{\Psi_0^2|\nabla\Psi_1|^2 + 2\Psi_0\Psi_1(\nabla\Psi_0 \cdot \nabla\Psi_1) + \Psi_1^2}, \\ f = n. \end{cases} \qquad (8)$$

For the factored transport equation (7), the Hamiltonian (3), with $u = A_1$, and forcing term are defined as:

$$\begin{cases} H = A_0(\Psi_0\nabla\Psi_1 + \Psi_1\nabla\Psi_0) \cdot \nabla A_1 \\ \quad +\big(\Psi_0\nabla\Psi_1 \cdot \nabla A_0 + A_0\nabla\Psi_0 \cdot \nabla\Psi_1 + \frac{1}{2}A_0\Psi_0\nabla^2\Psi_1\big)A_1, \\ f = 0. \end{cases} \qquad (9)$$

The Hamiltonian functions discussed thus far are used to compute the updated value of u in (3) ($u = \Psi_1$ for the factored eikonal equation and $u = A_1$ for the transport equation), denoted as u^{new}, which is then compared to its previous value, u^{old}, from the prior iteration. This iterative process continues until a specified threshold δ is satisfied. For brevity, the update rule, as detailed in [14], is omitted here.

In this approach, the factored Eikonal equation (8) is solved first, followed by the transport equation (9). The iterative procedure ensures accurate computation of the eikonal and of the amplitude. Finally, the electric field can be reconstructed as:

$$E(\mathbf{r}) = A(\mathbf{r})e^{-jk\Psi(\mathbf{r})}. \qquad (10)$$

The algorithm is straightforward to implement and surpasses ray tracing in terms of speed, simplicity, accuracy, and robustness. By solving the fundamental GO equations on a computational grid rather than along individual rays, it also accounts for diffraction effects arising from the shadow regions inherent in GO.

2.1 Maxwell Fish Eye Lens Analysis

We consider here an MFE lens [15], a spherical dielectric with a radius a and a radial refractive index defined by $n(r) = \frac{2}{1+(r/a)^2}$. The center of the sphere is at the origin. The phase distribution of the MFE lens is analytically determined, as both the rays and wavefronts follow arcs of circumferences and it is expressed as:

$$\Psi_{\text{MFE}}(\rho,z) = a\arccos\left(\frac{-2za}{\rho^2+z^2+a^2}\right). \qquad (11)$$

The amplitude of the electric field in the output of the half MFE lens ($z=0$), for a given radiation pattern $U(\theta) = \cos^3(\theta) = \left(\frac{a^2-\rho^2}{a^2+\rho^2}\right)^3$, is given by:

$$|\mathbf{E}(\rho)| = U(\theta)\frac{4a^2}{(a^2+\rho^2)^2} = \frac{4a^2(a^2-\rho^2)^3}{(a^2+\rho^2)^6}. \qquad (12)$$

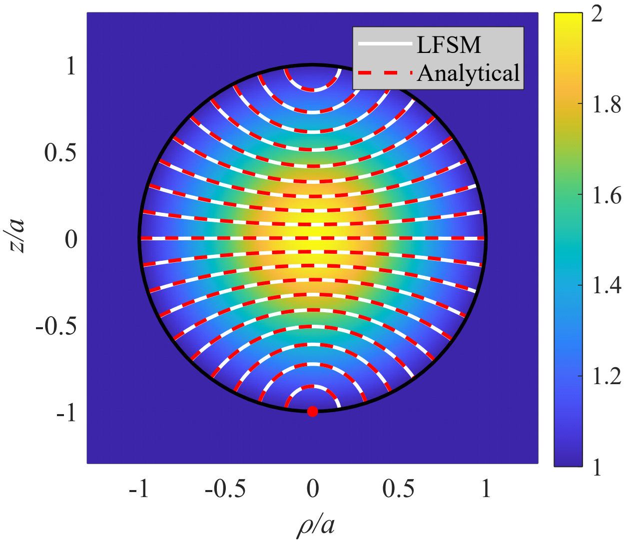

(a)

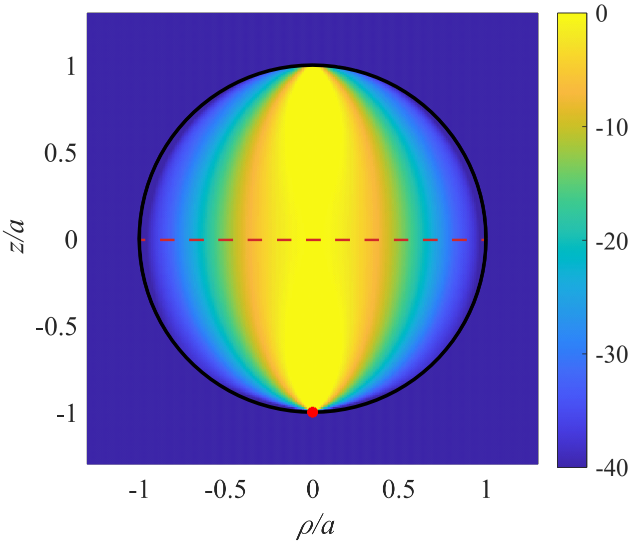

(b)

Figure 1. Phase distribution of MFE lens (a) calculated through the LFSM (white solid line) and the analytical formula (red dashed line). The source point is located at $\mathbf{r}_f = (0, -a)$. Amplitude distribution of a MFE lens (b) calculated through the LFSM, by considering a pattern described by $U(\theta) = \cos^3(\theta)$. The amplitude distribution in the red dashed line is compared to the analytical formula (12) in Fig. 2.

The 2D LFSM algorithm is initialized with a point source in free space at $\mathbf{r}_f = -a\hat{\mathbf{z}}$, where the Eikonal function in free space is defined as $\Psi_0 = \sqrt{\rho^2 + (z+a)^2}$. The initial amplitude is given by $A_0 = \cos^3(\theta)/\sqrt{\Psi_0}$. The chosen domain is $[-1.2, 1.2] \times [-1.2, 1.2]$ and the mesh 101×101. Fig. 1(a) shows a section of the MFE lens in a vertical plane, with the background color representing the refractive index, ranging from blue ($n = 1$) to yellow ($n = 2$). The surrounding medium beyond the MFE surface (black line) has a refractive index of $n = 1$. The wavefronts, computed using the LFSM (depicted as white solid lines), are compared to the analytical wavefronts (depicted as red dashed lines) obtained through (11). The two sets of trajectories exhibit perfect agreement, with a maximum error of approximately 10^{-6}. In Fig. 1(b), the amplitude of the MFE lens is depicted when illuminated by a feed located at $\mathbf{r}_f$ that emits radiation with an amplitude pattern proportional to $\cos^3(\theta)$. At $z = 0$, the amplitude computed using the LFSM (depicted as a red dashed line in Fig. 1(b)) is compared to the analytical formula in (12) and shown in Fig. 2. The results demonstrate excellent agreement between the two approaches. The computational time was about 0.9 seconds for the eikonal calculation, and about 1.2 seconds for the amplitude calculation, with a predefined threshold $\delta_\Psi = 10^{-6}$ for the eikonal and $\delta_A = 10^{-3}$ for the amplitude. The computational speed highly depends on the programming environment. We utilized `MATLAB Coder` to implement a `C++` version of the algorithm. Given that the algorithm requires four sweeps per iteration in 2D, resulting in multiple nested loops, `C++` is preferred for its efficiency in handling such operations.

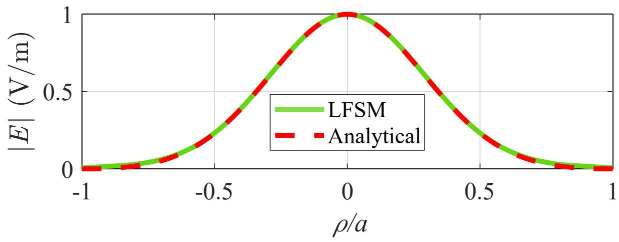

Figure 2. Amplitude distribution of the MFE lens in the output (red dashed line in Fig. 1(b)) retrieved through the LFSM (green solid line) and compared to the analytical one (red dashed line) from Equation 12.

3 Conclusions

This work presents a novel framework for the analysis of GRIN lens antennas, employing the Lax-Friedrichs Sweeping Method (LFSM) to efficiently solve the factored Eikonal and transport equations over a rectangular computational domain. The proposed approach offers several advantages over traditional ray tracing techniques, including faster computation, improved accuracy, and the ability to account for diffraction effects. These features make the LFSM an ideal tool for analyzing complex GRIN lens antenna systems. The effectiveness of the LFSM is demonstrated through the analysis of the Maxwell Fish Eye lens, achieving highly accurate results with significantly reduced computation time. Due to its rapid computation, the LFSM can be seamlessly integrated into optimization loops, functioning as a powerful design tool for GRIN lenses. Given a source and a desired complex aperture distribution on the output surface, this tool calculates the corresponding refractive index distribution, enabling the design of various types of inhomogeneous lenses.

Future research could focus on further improving the efficiency of the LFSM and extending its applicability to a wider range of GRIN lens configurations through optimization-driven methodologies.

References

[1] S. Zhang, R. K. Arya, S. Pandey, Y. Vardaxoglou, W. Whittow, and R. Mittra, "3d-printed planar graded index lenses," *IET Microwaves, Antennas & Propagation*, vol. 10, no. 13, pp. 1411–1419, 2016.

[2] S. Zhang, R. K. Arya, W. G. Whittow, D. Cadman, R. Mittra, and J. C. Vardaxoglou, "Ultra-wideband flat metamaterial grin lenses assisted with additive manufacturing technique," *IEEE Transactions on Antennas and Propagation*, vol. 69, no. 7, pp. 3788–3799, 2021.

[3] A. Paraskevopoulos, I. Gashi, M. Albani, and S. Maci, "High aperture efficiency 3d-printed radial grin lens," in *2022 16th European Conference on Antennas and Propagation (EuCAP)*, 2022, pp. 1–5.

[4] H. Xin and M. Liang, "3-d-printed microwave and thz devices using polymer jetting techniques," *Proceedings of the IEEE*, vol. 105, no. 4, pp. 737–755, 2017.

[5] H. F. Ma, B. G. Cai, T. X. Zhang, Y. Yang, W. X. Jiang, and T. J. Cui, "Three-dimensional gradient-index materials and their applications in microwave lens antennas," *IEEE Transactions on Antennas and Propagation*, vol. 61, no. 5, pp. 2561–2569, 2013.

[6] H.-X. Xu, G.-M. Wang, Z. Tao, and T. Cai, "An octave-bandwidth half maxwell fish-eye lens antenna using three-dimensional gradient-index fractal metamaterials," *IEEE Transactions on Antennas and Propagation*, vol. 62, no. 9, pp. 4823–4828, 2014.

[7] C. Mateo-Segura, A. Dyke, H. Dyke, S. Haq, and Y. Hao, "Flat luneburg lens via transformation optics for directive antenna applications," *IEEE Transactions on Antennas and Propagation*, vol. 62, no. 4, pp. 1945–1953, 2014.

[8] N. C. Garcia and J. D. Chisum, "High-efficiency, wideband grin lenses with intrinsically matched unit cells," *IEEE Transactions on Antennas and Propagation*, vol. 68, no. 8, pp. 5965–5977, 2020.

[9] A. Paraskevopoulos, F. Maggiorelli, M. Albani, and S. Maci, "Radial grin lenses based on the solution of a regularized ray congruence equation," *IEEE Transactions on Antennas and Propagation*, vol. 70, no. 2, pp. 888–899, 2022.

[10] F. Maggiorelli, A. Paraskevopoulos, J. C. Vardaxoglou, M. Albani, and S. Maci, "Profile inversion and closed form formulation of compact grin lenses," *IEEE Open Journal of Antennas and Propagation*, vol. 2, pp. 315–325, 2021.

[11] H. Zhao, "A fast sweeping method for eikonal equations," *Math. Comput.*, vol. 74, pp. 603–627, 2004. [Online]. Available: https://api.semanticscholar.org/CorpusID:16111206

[12] Y.-H. R. Tsai, L.-T. Cheng, S. Osher, and H.-K. Zhao, "Fast sweeping algorithms for a class of hamilton–jacobi equations," *SIAM Journal on Numerical Analysis*, vol. 41, no. 2, pp. 673–694, 2003.

[13] W. Chen, C.-S. Chou, and C.-Y. Kao, "Lax–friedrichs multigrid fast sweeping methods for steady state problems for hyperbolic conservation laws," *Journal of Scientific Computing*, vol. 64, pp. 591–618, 2015.

[14] S. Luo, J. Qian, and H. Zhao, "Higher-order schemes for 3D first-arrival traveltimes and amplitudes," *Geophysics*, vol. 77, no. 2, pp. T47–T56, 02 2012. [Online]. Available: https://doi.org/10.1190/geo2010-0363.1

[15] J. Maxwell, "Solution of problems. prob. 3, vol. viii, p.118," *The Cambridge and Dublin Mathematical Journal*, vol. IX, pp. 9–11, February 1854.